Journal of Aerosol Science 76 (2014) 13–27

Contents lists available at ScienceDirect

Journal of Aerosol Science

journal homepage: www.elsevier.com/locate/jaerosci

Chemical properties of insoluble precipitation residue particles

Jessie M. Creamean [a], Christopher Lee [b], Thomas C. Hill [c,1], Andrew P. Ault [d], Paul J. DeMott [e], Allen B. White [a], F. Martin Ralph [a,2], Kimberly A. Prather [b,f,*]

[a] Physical Sciences Division, National Oceanic and Atmospheric Administration/Earth System Research Laboratory, 325 Broadway R/PSD2, Boulder, CO 80305, USA
[b] Department of Chemistry and Biochemistry, University of California at San Diego, 9500 Gilman Dr., La Jolla, CA 92093, USA
[c] Department of Plant Sciences, University of Wyoming, Dept. 3354, 1000 E. University Ave., Laramie, WY 82071, USA
[d] Department of Environmental Health Sciences and Department of Chemistry, University of Michigan, 1415 Washington Heights, Ann Arbor, MI 48109, USA
[e] Department of Atmospheric Science, Colorado State University, 1371 Campus Delivery, Fort Collins, CO 80523, USA
[f] Scripps Institution of Oceanography, University of California, San Diego, 9500 Gilman Drive, La Jolla, CA 92093, USA

ARTICLE INFO

Article history:
Received 30 January 2014
Received in revised form
5 May 2014
Accepted 6 May 2014
Available online 21 May 2014

Keywords:
Precipitation chemistry
Insoluble residues
Soluble ions
ATOFMS
CalWater I
Ice nuclei

ABSTRACT

Precipitation chemistry can provide unique insights into the composition of aerosol particles involved in precipitation processes. Until recently, precipitation chemistry studies focused predominantly on soluble components. Analyzing the single particle insoluble components in addition to soluble ions in precipitation can provide detailed information on the individual particles originally in the cloud or removed by precipitation as well as the source of the aerosols. Herein, we present an in-depth analysis of resuspended residues from precipitation samples collected at a remote site in the Sierra Nevada Mountains in California during the 2009–2011 winter seasons. In addition, we present results from laboratory control experiments of dust, leaf litter, smoke, and sea salt samples that were conducted to better understand how insoluble and soluble residues are distributed during the atomization process and aid in the classification of the residue compositions in the precipitation samples. Further, immersion freezing ice nuclei (IN) measurements of insoluble residues from precipitation water enabled the determination of residue types that likely seeded clouds. Long-range transported dust mixed with biological material tended to be more IN active, while purely biological residues contained a variety of high and low temperature IN. Overall, results from this study can be used as a benchmark for classification of insoluble precipitation residues in future studies. Knowledge of the precipitation chemistry of insoluble residues coupled with meteorological and cloud microphysical measurements will ultimately improve our understanding of the link between aerosols, clouds, and precipitation.

* Corresponding author at: Department of Chemistry and Biochemistry, University of California at San Diego, 9500 Gilman Dr., La Jolla, CA 92093, USA. Tel.: +1 858 822 5312.
E-mail address: kprather@ucsd.edu (K.A. Prather).
[1] Present address: Department of Atmospheric Science, Colorado State University, 1371 Campus Delivery, Fort Collins, CO 80523, USA.
[2] Present address: Scripps Institution of Oceanography, University of California, San Diego, 9500 Gilman Drive, La Jolla, CA 92093, USA.

http://dx.doi.org/10.1016/j.jaerosci.2014.05.005
0021-8502/

1. Introduction

Aerosols serve as seeds for cloud droplet and ice crystal formation, and thereby their numbers and compositions can influence precipitation development (Pruppacher & Klett, 1978). Higher concentrations of cloud condensation nuclei (CCN) such as pollution aerosols are thought to suppress or delay the onset of precipitation (Rosenfeld, 2000), while aerosols, such as mineral and soil dust, can contain surface sites or properties that lead to their involvement as ice nuclei (IN) and are thought to enhance precipitation formation (Muhlbauer & Lohmann, 2009). Particles possessing properties that make them more effective as IN theoretically convert more water into precipitation, compared to CCN which actually slow the conversion of cloud drops into raindrops (Rosenfeld et al., 2008). Only a small portion of the available moisture in clouds is transformed into precipitation that reaches the surface (Bruintjes, 1999), demonstrating the importance of aerosols that convert available cloud moisture by serving as cloud nuclei. The overall effects of aerosols on precipitation formation and redistribution are highly uncertain (Huntington, 2006), highlighting the need for improved understanding of the sources and properties of aerosols that impact precipitation.

Laboratory studies of aerosols that serve as cloud nuclei and in-cloud measurements of aerosol chemical composition provide information regarding which types of aerosols selectively serve as IN or CCN (e.g., Creamean et al., 2013; Hao et al., 2013; Hegg et al., 2001; Hoose & Mohler, 2012; Pratt et al., 2009). For instance, sea salt particles have been shown to serve as efficient CCN but have relatively low efficiency as IN (DeMott et al., 2013; O'Dowd et al., 1997), while dust and biological aerosols have been shown to serve as both CCN and more efficient IN (Creamean et al., 2013; Rosenfeld et al., 2001; Sun & Ariya, 2006). Measurement of rainwater chemical composition is another approach for investigating aerosols as cloud nuclei; Levi and Rosenfeld (1996) found that Saharan dust had seeded clouds in Israel by measuring calcium ion concentrations in rainwater. Precipitation chemistry measurements provide additional information on how aerosols interact with precipitation, such as washout of boundary layer aerosols (Li et al., 2011), acidification of precipitation by urban pollution (Yang et al., 2012), and long-range transport of marine air masses impacting precipitation composition (Andreae et al., 1990). However, the majority of past studies either focused on the soluble and/or ionic components in a bulk mixture or involved small sample sizes, thus requiring assumptions to be made about the original, intact aerosols that interacted with the precipitation through cloud particle nucleation or scavenging. Few previous studies have focused on the insoluble, single particle components in cloudwater and precipitation (Ma et al., 2004; Matthias-Maser et al., 2000; Schutz & Kramer, 1987). Although these studies provided valuable information on the links between aerosols and precipitation, their sample sizes were limited.

IN are generally thought to be comprised of insoluble material (Field et al., 2006 and references therein). However, insoluble particles such as mineral dust can also serve as CCN if they acquire some amount of soluble material (e.g., ammonium sulfate), are cloud processed, or due to their typical size range, if their surface is wettable (Kumar et al., 2009; Rosenfeld et al., 2001). Thus, inspection of insoluble precipitation residues may provide insight into IN composition. Ault et al. (2011) and Creamean et al. (2013) utilized aerosol time-of-flight mass spectrometry (ATOFMS) to distinguish individual, insoluble precipitation residue particles such as dust, organic carbon from biomass burning, and biological material. Herein, we present more detailed chemical composition of precipitation samples collected during three winter sampling seasons of the CalWater I field campaign in the Californian Sierra Nevada Mountains (2009–2011), in addition to laboratory control experiments of known standards to serve as proxies for classification of the different types of residues observed in the rain and snow samples. Furthermore, filtered and heated measurements of immersion freezing IN concentrations in precipitation were made in an effort to determine which type of insoluble residues more likely served as IN. These analyses serve as a control study to help understand the sources of precipitation residue signatures, and to support analyses of insoluble residues from past and for future single particle insoluble residue classifications.

2. Materials and methods

2.1. Precipitation sample collection and analysis

Precipitation samples were collected during the CalWater I field campaign from 22 February to 11 March 2009 (10 samples total), 27 January to 15 March 2010 (21 samples total), and 28 January to 8 March 2011 (11 samples total) at a remote site, Sugar Pine Dam (SPD; 1064 m MSL; 39.13°N, 120.80°W), in the California Sierra Nevada. The start and end dates/times and number of residues analyzed by ATOFMS for each sample is provided in Table S1. Methods for collection and chemical analysis of precipitation residues are also described elsewhere (Ault et al., 2011; Creamean et al., 2013; Holecek et al., 2007). Precipitation samples were manually collected using beakers cleaned with ultrapure Milli-Q water (18 MΩ cm^{-1}) and methanol. Most samples were analyzed immediately after collection, while others were transferred to 500-mL glass bottles, frozen, and stored for 6–10 days before chemical analysis. Residues in the precipitation samples were resuspended in dry air using a Collison atomizer, dried using two silica gel diffusion driers, and sampled by ATOFMS. This aerosolization method can produce single soluble and insoluble particles as well as agglomerates of different particle types. In addition, soluble species can coat insoluble residues, and thus the composition is somewhat altered from the original compositions as dry suspended aerosols (Holecek et al., 2007). Additional caveats associated with residue composition as a result of this method are discussed in the following sections. Despite caveats, this method has provided useful information on the composition of precipitation particles (Ault et al., 2011; Creamean et al., 2013).

ATOFMS measures the size and chemical composition of individual particles/residues in real time (Gard et al., 1997). Briefly, particles are pulled through a differentially pumped vacuum chamber then individually sized by passing through two 532-nm, continuous wave Nd:YAG lasers spaced a set distance apart. The particles are then desorbed and ionized by a pulsed 266-nm Nd:YAG laser, where positive and negative ions are generated and analyzed in the dual polarity mass spectrometer chamber. Particle mass spectra were manually inspected and classified based on combinations of characteristic ion peaks in both negative and positive spectra. In order to be classified as a particular residue type, the mass spectrum of the residue must contain a specific combination of ions; the combinations of ions used for classification are based on those previously measured in precipitation samples using ATOFMS (Ault et al., 2011; Creamean et al., 2013; Holecek et al., 2007). Note that classification labels do not reflect all of the species present within a specific residue, but reflect a distinct mass spectral pattern common to single particle spectra of this residue type.

2.2. Control experimentation sample preparation and analysis

Dry materials chosen for control experiments were based on the types of residues detected in precipitation samples during CalWater I and are provided in Table S2, along with the number of residues analyzed by ATOFMS for each sample. Solutions were prepared by suspending a small quantity of dry control experiment material ($\sim$0.1–1.6 g) in $\sim$100–200 mL of Milli-Q. The goal was to reproduce the environment of the precipitation residues, i.e., a dilute, aqueous environment. Suspended control solutions were aerosolized and analyzed using ATOFMS, similar to the precipitation samples. Control experiment analysis may produce insoluble and soluble residues depending on the concentration of the soluble material in solution, as discussed in the Supplementary Material (SM) and in Section 3.1.

Dust samples include laboratory standards and samples collected in the field. Mineral dust samples included Arizona Test Dust (ATD; Powder Technology Inc.), obtained from milling of naturally occurring sand in Arizona, U.S., and laboratory-produced kaolin (Sigma Aldrich®). Elemental composition analysis of ATD shows the following minerals, in order of abundance: silicon (79.1%), aluminum (8.2%), calcium (4.0%), sodium (2.3%), iron (2.2%), magnesium (2.1%), and potassium (1.7%) (Vlasenko et al., 2005). Soluble anions observed by Vlasenko et al. (2005) in resuspended ATD included sulfate (41 $\mu g\, m^{-3}$) and phosphate (3 $\mu g\, m^{-3}$), with minor contributions from fluoride, acetate, formate, chloride, and nitrate ($\leq$0.5 $\mu g\, m^{-3}$). Kaolin is predominantly composed of kaolinite (aluminum silicate hydroxide, $Al_2Si_2O_5(OH)_4$), but also has trace amounts ($\leq$1.5%) of iron(III) oxide, titanium dioxide, calcium oxide, magnesium oxide, potassium oxide, sodium oxide, and manganese(III) oxide. Soil samples collected from the top 1–2 cm of the ground at SPD and from sand dunes at two locations in Gansu, China were also analyzed. The Gansu soil samples were collected from Dunhuang ("Asian 1") and YaDan National Geological Park ("Asian 2"). After initial aerosolization and analysis, the ATD, Asian 1, and Asian 2 solutions were stored in sealed jars and left at room temperature for 22–29 days to enable possible growth from biological material present in the soil, then reanalyzed with ATOFMS (herein referred to as the 'aqueous growth' experiments). Our method is validated by results from the aqueous growth experiments, which are shown and discussed in the SM. The presence of biological material in control experiment dust samples are also shown and discussed in detail in the SM.

Eucalyptus leaves from the University of California, San Diego (UCSD) campus were used as a proxy for biogenic signatures, which, while not from the same species present at SPD, provide useful insight as to the signatures of large scale florae. Previous laboratory experiments of biota samples, including leaf litter, were also used as a proxy for classification of biological precipitation residues (Silva, 2000). To simulate biomass burning, dry leaf litter from UCSD was combusted in an Erlenmeyer flask. The smoke from the smoldering leaf litter was collected in a second Erlenmeyer flask, which was sealed until the smoke settled. Milli-Q water was then added to the sealed flask and immediately aerosolized for ATOFMS analysis. Previous ATOFMS biomass burning chemical signatures were used as a proxy to classify the precipitation residues (e.g., Silva et al., 1999); however, this control experiment represents the first ATOFMS laboratory measurements of a biomass burning species present in an aqueous medium.

Sea salts (SS; Sigma Aldrich®) were analyzed separately and as a mixture with ATD. SS is an artificial mixture closely resembling the composition of dissolved inorganic salts in ocean water and is predominantly composed of sodium and chloride (10,780 mg L^{-1} and 19,290 mg L^{-1}, respectively), with smaller contributions from sulfate, potassium, calcium, carbonate, strontium, boron, bromide, iodide, lithium, fluoride, and magnesium (all $<$2660 mg L^{-1}). After the initial analysis, half of the SS solution was mixed with half of the ATD solution (denoted as "SS+ATD"). After vigorous mixing, the SS+ATD solution was aerosolized and analyzed using ATOFMS. The goal of using mixed solutions from the control experiment was to better understand specific signatures of dust residues from the precipitation samples collected at SPD and to determine if agglomerates and coatings from sea spray aerosol (SSA) formed on the dust, for instance during transport over the Pacific Ocean (Sullivan et al., 2007a, 2007b).

Initially, single particle mass spectra from each control experiment were imported into YAADA (Allen, 2004), a software toolkit for Matlab (The Mathworks, Inc.). An adaptive resonance theory-based clustering algorithm (ART-2a) (Song et al., 1999) was then used to group single particle mass spectra into clusters based upon similarities in the presence and intensity of ion peaks. The ART-2a-identified clusters accounted for $>$90% of the total residues analyzed by ATOFMS. ART-2a was run separately on each control experiment, since residues from the individual experiments were similar, i.e., not a mixture of different residue types such as the precipitation samples. Spectra for each control experiment represent averages of $>$90% of all the residues analyzed (with a small number of spectra excluded that were not matched to the clusters, e.g., spectra that did not have a positive mass spectrum), while precipitation residue mass spectra shown are each from a single,

representative residue. Thus, the control experiment and precipitation residue spectra will not look identical, but contain similar ions.

2.3. Soluble species experiments

Ion chromatography (IC) was performed on precipitation samples from 2009 to determine the soluble species present. Analysis for select soluble cations (Li^+, Na^+, K^+, Ca^{2+}, NH_4^+) and anions (Cl^-, SO_4^{2-}, NO_3^-, PO_4^{3-}) was performed using a Metrohm Ion Chromatograph equipped with a 100 μL injection loop, an 820 IC separation center, an 819 IC detector, a Metrosep C2 100 100 × 4 mm–7 mm cation column, and a Metrosep A Supp5 100/4.0 mm anion column with an 853 CO_2 suppressor. Samples were prepared by acquiring 10-mL aliquots of precipitation samples. Detector settings and standards were used as a calibration to convert from ion peak area to ppb. Concentrations are presented in μmol L^{-1} (μM). Blank samples were analyzed from Milli-Q water that was added to a glass bottle, similar to what the precipitation samples were stored in. Size distributions of aerosol produced from solutions of various concentrations of artificial SS were measured to demonstrate why soluble species are observable by the ATOFMS in the control experiments but not in collected precipitation samples. Methods are discussed in the SM.

2.4. Ice nuclei measurements

Ice nuclei (IN) measurements provided additional information regarding the climate-relevant properties of the precipitation residues. Precipitation samples were analyzed for IN via immersion freezing directly after melting, and after concentrating insoluble matter by filtering through a 0.2 μm pore diameter polycarbonate nuclepore filter (Whatman) followed by resuspension in a small aliquot of the filtrate. Immersion freezing of IN is relevant for wintertime mixed-phase clouds where supercooled liquid is present (Murray et al., 2012 and references therein), such as those observed during CalWater. Filter concentration increased the sensitivity of detection of IN that were active at warmer temperatures. For the Asian soil samples, 2 g of air dry material was suspended in 10–50 mL deionized water, shaken at 400 rpm on a rotary shaker for 20 min, and then this suspension, and serial dilutions of it, were tested. The kaolin used as a comparator with the soils was type KGa-1b (97% kaolinite, from the Clay Minerals Society). IN number concentrations active by immersion freezing were estimated for a select set of precipitation samples (per mL) and the Asian soil (per g suspended in Milli-Q water) samples by counting the number of 50 or 80 μL aliquots (n=32–96) of precipitation water or dust suspensions frozen in 96-well polypropylene polymerase chain reaction (PCR) trays (Garcia et al., 2012). Trays were cooled to −9.0 °C in a thermal cycler (PTC-200, MJ Research, Waltham, MA) descending in 1 °C increments, and then in 96-well aluminum incubation blocks to −20 °C. Each temperature step during cooling was held stable for 5 min before counting the wells. Cumulative numbers of IN per mL re-suspension water were estimated using formula $-\ln(f)/V$, where f is the proportion of droplets not frozen and V is the volume of each aliquot (Vali, 1971). After initial testing, samples were heated to 95 °C for 20 min while suspended in deionized water to denature and inactivate certain biological sources of IN such as ice nucleating proteins in IN active bacteria (Christner et al., 2008b; Conen et al., 2011).

3. Results and discussion

3.1. Chemical composition of precipitation residues

Figure 1 shows individual representative mass spectra for each of the different insoluble residue types from the CalWater I precipitation samples (Creamean et al., 2013). Dust residues varied in mineralogy, but typically contained a combination of the metal and metal oxides ($^{23}Na^+$, $^{27}Al^+$, $^{39,41}K^+$, $^{40}Ca^+$, $^{48}Ti^+$, $^{54,5}Fe^+$, $^{64}TiO^+$) shown in the positive mass spectra in Fig. 1a ("Dust 1") and Fig. 1b ("Dust 2"), while the negative mass spectra contained ion peaks for aluminosilicates ($^{43}AlO^-$, $^{59}AlO_2^-$, $^{60}SiO_2^-$, $^{76}SiO_3^-$) and/or biological ions (organic nitrogen and phosphorus; $^{26}CN^-$, $^{42}CNO^-$, $^{63}PO_2^-$, $^{79}PO_3^-$, $^{97}PO_4^-$) (Pratt et al., 2009; Sullivan et al., 2007a). In order for a residue to be classified as containing biological material, all of the aforementioned biological ions must be present. While it is possible the phosphorus ion markers could originate from phosphate dust minerals, we assume the phosphorus ion markers originate from biological material if they are present with the organonitrogen markers ($^{26}CN^-$, $^{42}CNO^-$) in the same particle, as in the case with the precipitation residues from CalWater I. However, dust particles analyzed by ATOFMS can contain phosphorus ion markers without organonitrogen, such as kaolin (Fig. 3d), in which case the phosphorus ions are likely not of biological origin. Purely dust residues were rarely observed in the precipitation samples; the dust in precipitation could have originally been pure dust which developed a biological coating during aerosolization or, more likely, could have originally been dust mixed with biological material (Creamean et al., 2013). A unique dust subtype, calcium-rich dust, is shown in Fig. 1c which was classified by calcium ions ($^{40}Ca^+$, $^{56}CaO^+$, $^{57}CaOH^+$, $^{84}Ca_2^+$, $^{96}Ca_2O^+$, $^{113}(CaO)_2H^+$). These residues contained sulfur-related ions in the negative mass spectra ($^{64}SO_2^-$, $^{80}SO_3^-$), in addition to higher mass aluminosilicate ions ($^{119,120,121}AlSiO_4^-$, $^{136}Si_2O_5^-$, $^{137}HSi_2O_5^-$, $^{148,149,150}Si_3O_4^-$; shown in inset).

Biological residues in the precipitation samples contained ion combinations similar to those previously observed in precipitation residues (Holecek et al., 2007) and cloud ice crystals (Creamean et al., 2013; Pratt et al., 2009; Suski et al., 2014; Suski, 2014). Our definition of biological residue particles may differ than those defined elsewhere using other techniques

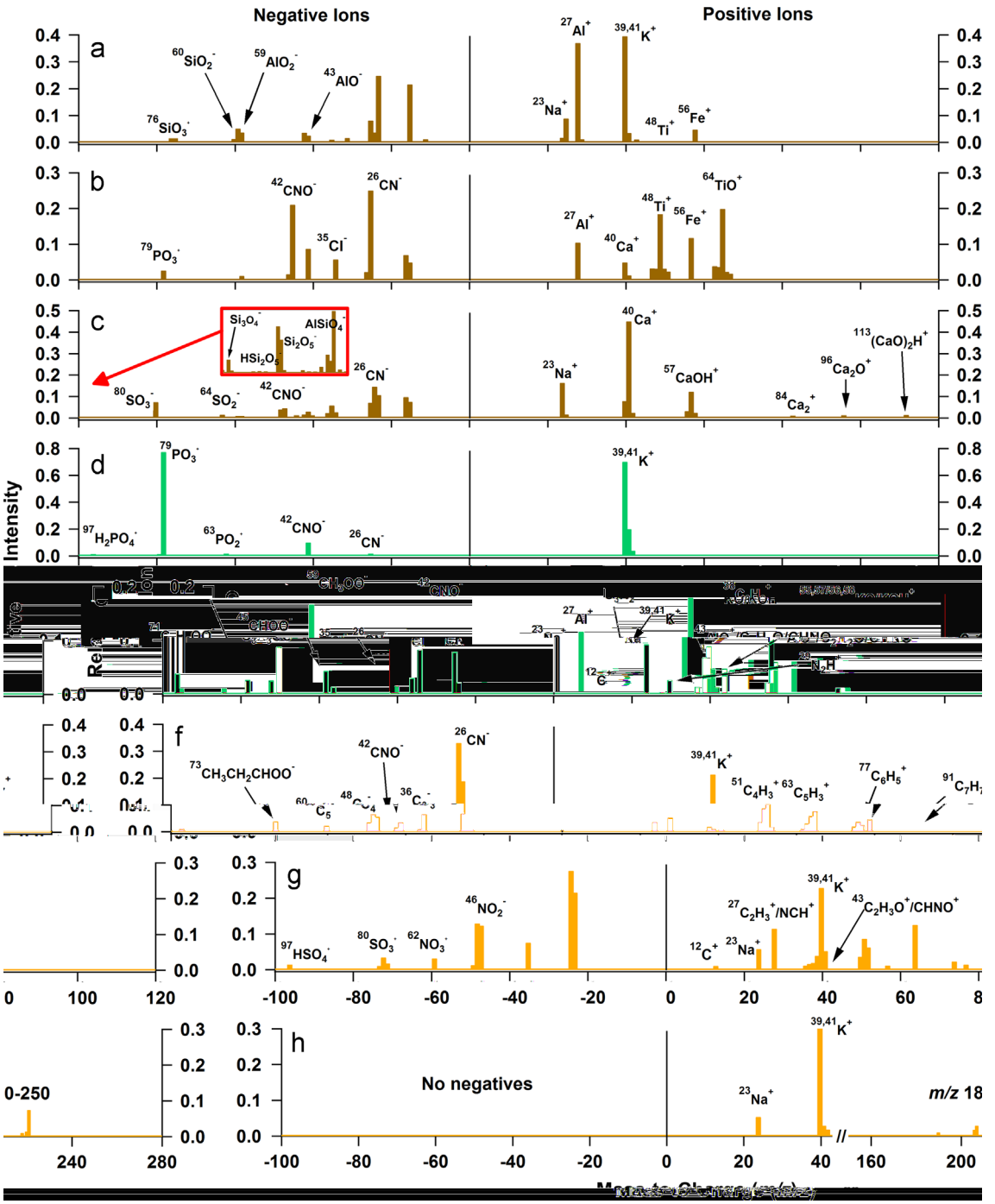

Fig. 1. Representative ATOFMS mass spectra for individual insoluble residues from precipitation samples collected at Sugar Pine (SPD) during CalWater I. Each spectrum is from a single residue that was representative of the combination of ions used to classify each precipitation residue type. Examples include different dust (a–c), biological (d and e), and OC residues (f–h). The inset for (c) shows a magnified portion of the dust spectrum that contains the high mass aluminosilicate ions ($^{119,120,121}AlSiO_4^-$, $^{136}Si_2O_5^-$, $^{137}HSi_2O_5^-$, $^{148,149,150}Si_3O_4^-$). (a) Dust 1, (b) dust 2, (c) Ca-rich dust, (d) Bio 1, (e) Bio 2 (f) OC-aromatic, (g) OC (with Na and K) and (h) OC (PAH).

(e.g., Jaenicke, 2005), where biological particles are often defined as particles containing cellular material. The mass spectral signatures of "biological residues" can be differentiated from dust residues containing biological material (i.e., Dust 2) on the basis of abundant organic, phosphorus, and/or organic nitrogen ions, as well as a lack of key dust markers such as aluminosilicates and titanium (Pratt et al., 2009). The first biological type contained the combination of ions shown in Fig. 1d and herein referred to as "Bio 1". The second biological type is shown in Fig. 1e and is herein called "Bio 2". The ions in Bio 2

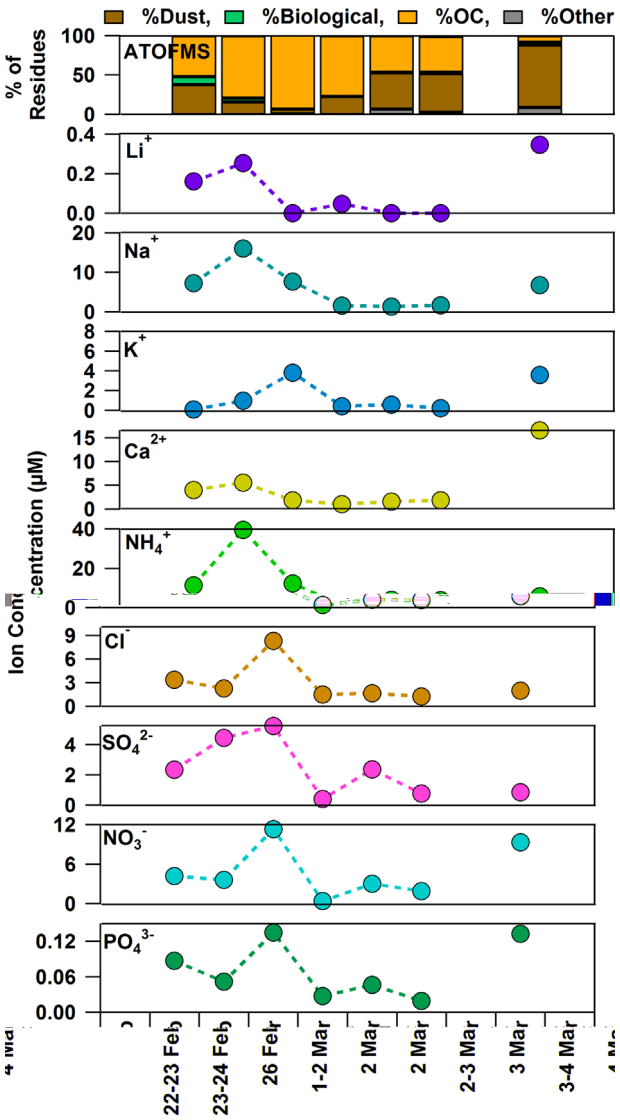

Fig. 2. Insoluble and soluble chemical analysis from the 2009 precipitation samples. Top panel shows ATOFMS residues from 2009 precipitation samples. Remaining panels show results from soluble ions measured from ion chromatography (IC). Samples from 22 to 23 February, 3 and 4 March were not included in soluble ion analysis because no unaerosolized sample was left after ATOFMS analysis.

were similar to those of Bio 1 with additional contribution from potassium ions ($^{55,57}KO^+$, $^{56,58}KOH^+$), chloride ($^{35,37}Cl^-$), and organic carbon ions ($^{45}CHOO^-$, $^{59}CH_3COO^-$, $^{71}C_3H_3OO^-$, $^{73}CH_3CH_2CHOO^-$) (Sullivan & Prather, 2007). While $^{35,37}Cl^-$ and $^{71}C_3H_3OO^-$ have been observed in biological mass spectra from previous studies (e.g., Fergenson et al., 2004; Silva, 2000), organic acids such as formic (CHOOH) and acetic (CH_3COOH) acids are normal constituents of leaf litter (Hongve et al., 2000), and have also been shown to be biodegradation products largely present in cloudwater (Vaïtilingom et al., 2010). Further, chloride and the organic ions in Bio 2 have been observed in biomass burning aerosols (Silva et al., 1999), suggesting this residue type could be from biomass burning. Previous work has shown that biological aerosols can also be composed of insoluble organics in marine atmospheres (Facchini et al., 2008; Spracklen et al., 2008), however they can also contain soluble materials such as organic acids, mycotoxins, antigens, and endotoxins (Burge & Solomon, 1987; Kumar et al., 2003).

Organic carbon (OC) residues consisted of three main types as shown in Fig. 1f is the OC-aromatic (OC with aromatic fragment ions at $^{51}C_4H_3^+$, $^{63}C_5H_3^+$, $^{77}C_6H_5^+$, and $^{91}C_7H_7^+$), Fig. 1g is the OC enriched with Na^+ and K^+, and Fig. 1h is the polycyclic aromatic hydrocarbons (PAHs, high mass OC ions between *m*/*z* 180–250). These species most likely originated from biomass burning aerosols and were dissolved/transformed during the atomization process (Ault et al., 2011; Holecek et al., 2007; Petters et al., 2009; Qin & Prather, 2006). Negative ion mass spectra for the OC types typically contained organic nitrogen and organic carbon ions. The negative mass spectra also contained soluble species including nitrate ($^{46}NO_2^-$, $^{62}NO_3^-$) and sulfate ($^{97}HSO_4^-$). Nitrate and sulfate may be incorporated into the insoluble residues through encasement in an insoluble organic shell, which has been observed in biomass burning aerosols (Moffet et al., 2010; Pósfai et al., 2004), and/or

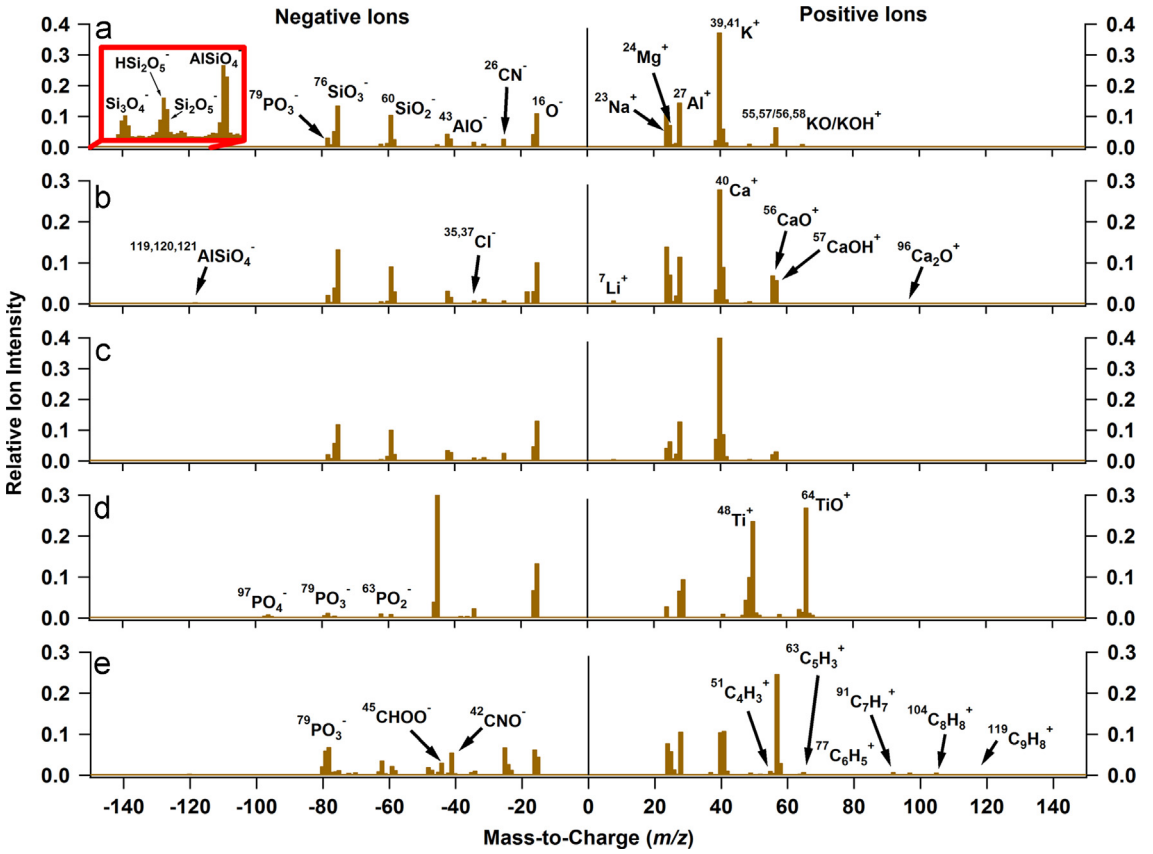

Fig. 3. Average ATOFMS mass spectra for residues from the dust control experiment solutions (> 90% of the total residues analyzed). The inset shows a magnified portion of the dust spectrum that contains the high mass aluminosilicate ions ($^{119,120,121}AlSiO_4^-$, $^{136}Si_2O_5^-$, $^{137}HSi_2O_5^-$, $^{148,149,150}Si_3O_4^-$). (a) ATD, (b) Asian 1, (c) Asian 2, (d) Kaolin, (e) SPD Soil.

dissolution in the precipitation solution followed by coating of the insoluble residues upon aerosolization (Holecek et al., 2007).

Figure 2 shows the overall composition from ATOFMS chemical classifications of insoluble residues (top panel) in addition to soluble species from ion chromatography (IC) measurements of the 2009 precipitation samples (bottom panels). Overall, concentrations of the anions and cations are consistent with previous precipitation chemistry measurements of soluble species worldwide (Sun et al., 2010 and references therein). The precipitation sample containing the most insoluble dust residues (3–4 March, 2009) corresponded to the largest concentration of soluble Ca^{2+}; high calcium content in precipitation has previously been attributed to dust (Brahney et al., 2013; Levi & Rosenfeld, 1996; Noguchi & Hara, 2004). In contrast, the precipitation containing the most insoluble OC (1–2 March, 2009) corresponded to the largest concentrations of soluble SO_4^{2-} and Cl^-; both species likely from biomass burning. However, both the dust and OC samples contained large, comparable concentrations of soluble K^+, PO_4^{3-}, and NO_3^-. Thus, measurements of bulk soluble ions, alone, cannot distinguish specific types of particles present in the precipitation.

3.2. Chemical signatures of control experiments

3.2.1. Dust chemical signatures

ATOFMS spectra of dust contain a plethora of various metals and metal oxides, as discussed in Section 3.1 for the precipitation residues. The dust control experiments provided valuable insight into the species present in dust precipitation residues. Figure 3 shows average mass spectra from the control experiments of the dust suspensions. Many common ions are present within both the precipitation samples and the different standards in Fig. 3. For instance, ATD, Asian 1, and Asian 2 (Fig. 3a–c) contain the same aluminosilicate ions as the dust precipitation residue shown in Fig. 1a. Further, kaolin (Fig. 3d) has similar ions to the dust precipitation residue shown in Fig. 1b, including $^{27}Al^+$, $^{40}Ca^+$, $^{48}Ti^+$, $^{54,56}Fe^+$, and $^{64}TiO^+$. Calcium ions present in the calcium-rich dust precipitation residues (Fig. 1c) were also present in dust control experiments, particularly in the Asian 1 and 2 samples, and are likely from calcium carbonate ($CaCO_3$) (Sullivan et al., 2007a). The $^{60}CO_3^-$ ion was not observed in the any of the dust mass spectra because $CaCO_3^+$ predominantly fragments to CaO^+ and $CO_{2(g)}$ using the ATOFMS laser desorption/ionization method (Sullivan et al., 2009b, 2010). The Asian 1 and 2 soil samples were collected

near the Chinese Loess Plateau, where the dust has been shown to be rich in calcium carbonate (Krueger et al., 2004; Sullivan et al., 2007a). Calcium has also been observed in surface snow on a glacier in Asia and was attributed to gypsum and calcite from the surrounding deserts (Zhang et al., 2013). Interestingly, Creamean et al. (2013) showed air mass transport from over Asia during the same time period with the highest percentages of calcium-rich dust residues in the precipitation collected in 2011 (14–16 February). Most of the control experiment dust samples contained the higher mass aluminosilicate ions (shown in Fig. 3a inset), which were also observed on the calcium-rich dust in the precipitation samples. The main difference between the Asian 1 and 2 soil samples and the calcium-rich dust precipitation residues were the sulfur-related ions ($^{64}SO_2^-$, $^{80}SO_3^-$). The sulfur-related ions were typically consistent with sulfate ($^{97}HSO_4^-$) in the precipitation samples, except when samples contained large percentages of calcium-rich dust residues, as shown and discussed in more detail in the SM. The sulfur-related ions were omnipresent and particularly abundant in the calcium-rich dust precipitation residues, but occasionally nitrate and organic ions were observed in the negative mass spectra as well (Fig. S4). This suggests that sulfate was originally mixed with the calcium-rich dust residues, while the nitrate and organic species are a result of a soluble coating from the aerosolization process. It is also possible that some contribution of nitrate and organic species could also be a result of cloud and heterogeneous processing of the dust (Sullivan et al., 2007a, 2009a; Sullivan & Prather, 2007). Several studies have shown that gypsum ($CaSO_4 \cdot 2H_2O$) is a product of calcite dust aerosols ($CaCO_3$) reacting with SO_2 during transport (Okada et al., 1990; Rosenfeld et al., 2001 and references therein). Thus, the calcium-rich dust was potentially $CaCO_3$ transported from the Loess Plateau region and chemically transformed by SO_2 during transport over Asia (Dentener et al., 1996; Dunlea et al., 2009; Sullivan et al., 2007a). However, there is still the possibility that some sulfate could also be a result of a coating formed during the aerosolization process.

The only control experiment of dust that contained ions that were not observed in the dust precipitation residues was the SPD soil. As shown in Fig. 3e, some of the residues from the SPD soil sample contained organic nitrogen and organic carbon ions ($^{51}C_4H_3^+$, $^{63}C_5H_3^+$, $^{77}C_6H_5^+$, $^{91}C_7H_7^+$, $^{45}CHOO^-$, $^{59}CH_3OO^-$, and/or $^{71}C_3H_3OO^-$) that were actually present in Bio 2 (Fig. 1e) and OC (Fig. 1f) precipitation residues, although the SPD soil is not an exact fingerprint of either the Bio 2 or OC precipitation residues. Soil in remote forested areas tends to have a higher organic matter content compared to desert soils (Fernandez et al., 1997; Schnitzer & Khan, 1978). Therefore, SPD soil would be expected to contain more organic species compared to dust from arid regions. However, not all spectra from SPD soil contained the organic nitrogen and carbon ions; 34% of the SPD soil residues were similar to the other dust control experiments. The fact that the SPD soil was not similar to the dust residues in the precipitation provides a strong indication that the dust in the precipitation was not local, providing additional support for the importance of long-range transport to precipitation over California (Creamean et al., 2013).

3.2.2. Vegetation and biomass burning chemical markers

To probe the connection to the components in biomass burning aerosols, average mass spectra from the leaf litter (a) and leaf litter smoke (b) control experiment are shown in Fig. 4. Leaf litter contained mainly $^{23}Na^+$ and $^{39,41}K^+$ in the positive mass spectra, while the negative mass spectra contained phosphorus ions, organic carbon ions, and chloride. The positive ion mass spectra for leaf litter were similar to the Bio 1 residue type, while the negative ion mass spectra were similar to Bio 2. After the leaf litter was ignited, combusted, and analyzed, the spectra changed considerably (Fig. 4b), as expected, and is similar to that of the OC precipitation residue shown in Fig. 1g. The negative mass spectra contained chloride, nitrate, and sulfate (intense $^{80}SO_3^-$ and $^{97}HSO_4^-$), which have previously been observed in biomass burning particles by ATOFMS (e.g., Qin & Prather, 2006; Silva et al., 1999). Further, the inset shows a magnified region of the leaf litter smoke positive ion mass spectra, which contain ions for high mass organic carbon (HMOC) (Qin & Prather, 2006). HMOC ions were occasionally observed in the precipitation residues (up to 50% and average of ~11% out of all OC residues, not shown in Fig. 1), suggesting the biomass burning residues in the precipitation may have contained ions for HMOC in an organic coating from aqueous phase processing (Moffet et al., 2010; Qin & Prather, 2006).

3.2.3. Sea salt chemical markers and mixtures

Previous studies have shown that dust can become internally mixed with sea spray aerosol (SSA) during transport over the oceans (Andreae et al., 1986; Sullivan et al., 2007a, 2007b). SS residues, alone, were not observed in the precipitation samples collected during CalWater I. However, SS species were mixed in dust residues as discussed in Section 3.3. Although SS is thought to dissolve in precipitation samples, control experiments show that SS residues are formed and can be measured when the solution solute concentration becomes high enough (shown in Fig. S5 and discussed further in the SM). Sea salt is soluble, yet when aerosolized and dried for ATOFMS analysis, produces agglomerates of the soluble species to form particles. When the concentration of SS is low, the residue sizes are too small for the ATOFMS to detect; however, as the concentration increases, eventually the residues become large enough to detect. Figure 5a shows the average mass spectrum from the SS control experiment. Common SS ions include $^{23}Na^+$, $^{24}Mg^+$, $^{35,37}Cl^-$, and sodium chloride clusters ($^{81,83}Na_2Cl^+$, $^{93,95,97}NaCl_2^-$) (Gaston et al., 2011; Prather et al., 2013). Sea salt was observed in cloud residues during simultaneous aircraft and ground measurements during the 2011 CalWater I sampling, but not in precipitation collected at the same time as the flights, due to the strong dilution of sea salt in the precipitation samples (Creamean et al., 2013). The concentration of the SS control experiment solution was approximately 45% that of seawater (15.7 g L^{-1}), corresponding to 208.9 and 242.5 mM of Na^+ and Cl^-, respectively. The concentrations of SS in the precipitation samples were much lower due to the dilution of individual SSA particles in raindrops: Fig. 2 shows concentrations of 1.3–16.1 and 1.3–8.3 μM for Na^+ and Cl^-, respectively, for precipitation samples from 2009. When the SS solution was mixed with the ATD solution and

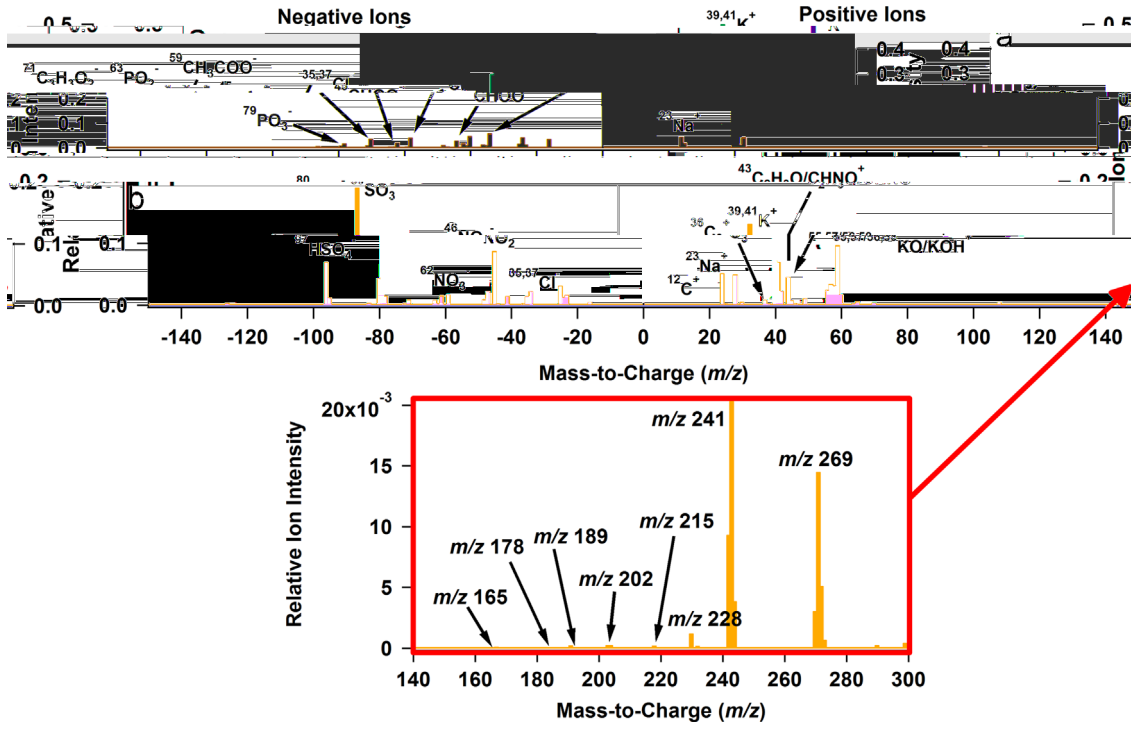

Fig. 4. Average ATOFMS mass spectra for residues in the leaf litter and leaf litter smoke control experiment samples (> 90% of the total residues analyzed). Magnified region of the leaf litter smoke positive mass spectra (*m/z* range not shown in (b)), which displays HMOC ions, is shown in the red box. (a) Leaf Litter and (b) Leaf Litter Smoke. (For interpretation of the references to color in this figure legend, the reader is referred to the web version of this article.)

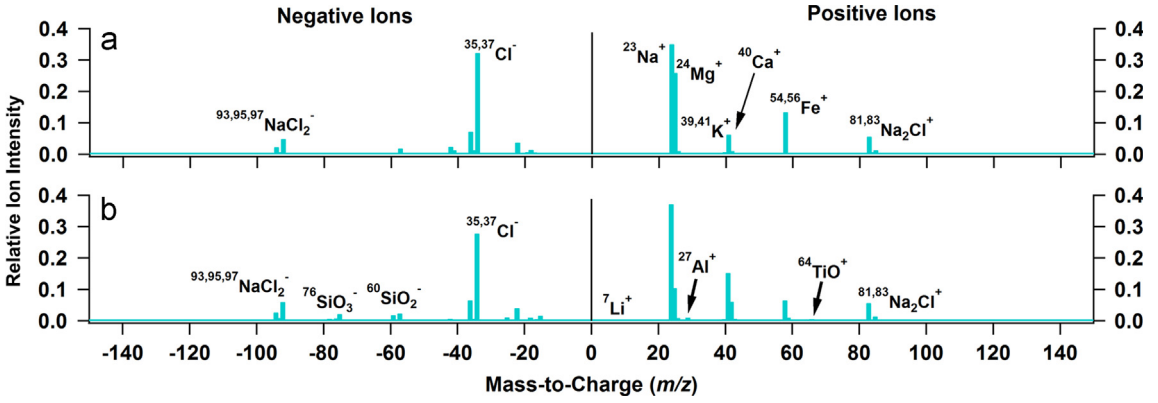

Fig. 5. Average ATOFMS mass spectra for residues in the artificial sea salts (SS) and SS+ATD mixture control experiment samples (> 90% of the total residues analyzed). (a) Artificial Sea Salts and (b) Artificial Sea Salts + ATD.

immediately aerosolized for ATOFMS analysis, 34% of the residues showed mixing of the dust and SS ions (i.e., single residues that contained both $^{35}Cl^-$ and $^{76}SiO_3{}^-$). Figure 5b shows the residues that contained both dust and SS ions. Aluminosilicate, titanium, and lithium dust ions were observed, in addition to $^{35,37}Cl^-$, $^{81,83}Na_2Cl^+$, and $^{93,95,97}NaCl_2{}^+$. Thus, dust has the potential to mix with sea salt in the atmosphere, which is discussed in more detail in Section 3.3.

3.3. *Detailed chemical analysis of precipitation samples from CalWater I*

Based on control experiment results, key ions were investigated for their occurrence and abundance in the precipitation sample residues. Figure 6 shows a compilation of the chemical compositions of the residue types (top row) and select ions (bottom two rows) averaged from all residues analyzed during each winter sampling season of CalWater I. Ions shown were selected based on minimal interference from other ions of the same *m/z* and if their differences between each year was statistically significant (Student's *t*-test; $p < 0.05$). Unless noted otherwise, all differences between the relative ion peaks areas in samples each year was statistically significant. The purpose of Fig. 6 is to show the range of the residue percentages

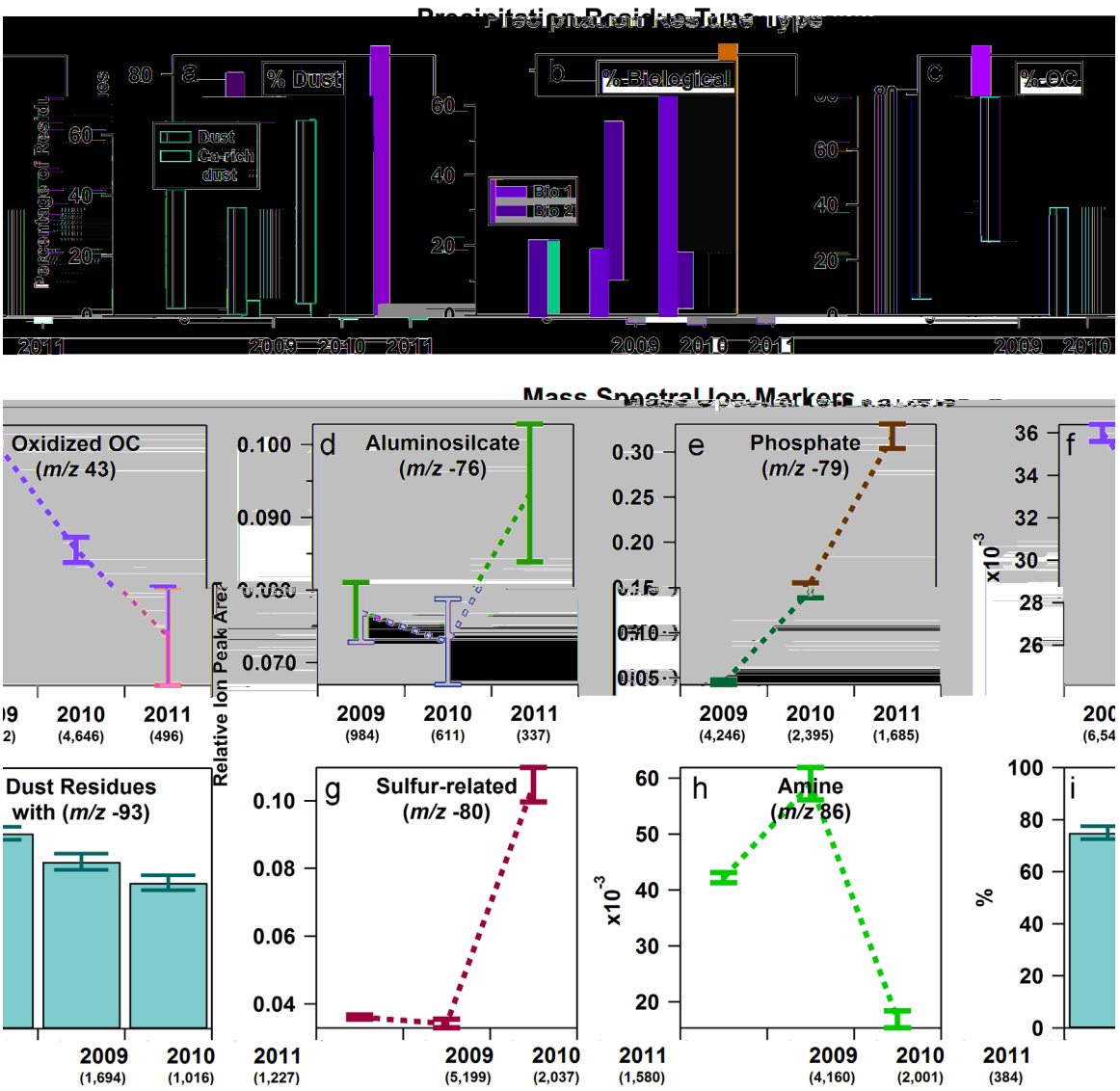

Fig. 6. Summary of insoluble ATOFMS analysis from the three winter sampling seasons (2009–2011) of CalWater I. Top row shows the different precipitation residue types for (a) dust, (b) biological, and (c) OC. The bars represent the range of the percentage of each type of residue per sample. Note that the "%Dust" is separated into the calcium-rich dust and all other dust (i.e., Dust 1 and Dust 2), and the "% Biological" is separated into Bio 1 and Bio 2. These bars are slightly offset to show overlapping regions. The bottom two rows show the relative ion peak area of (d) aluminosilicate ($^{76}SiO_3^-$), (e) phosphate ($^{79}PO_3^-$), (f) oxidized OC ($^{43}C_2H_3O/CHNO^+$), (g) sulfur-related ion ($^{80}SiO_3^-$), (h) sodium chloride cluster ($^{83}Na_2Cl^+$), and (i) amine ($^{86}C_2H_2/(C_2H_5)_2NCH_2^+$) of each precipitation sample collected during each winter sampling seasons. The bars for each year represent the 95% confidence interval of the average relative ion peak area. The number of particles containing each *m/z* is provided in parentheses per year.

per precipitation sample and relative ion peak areas of commonly observed species, in addition to a general comparison between the winter sampling seasons.

The aluminosilicate ion had trends consistent with the percentages of dust residues, demonstrating their utility as proxies for dust, as particularly shown during the 2011 samples. The difference between the aluminosilicate relative ion peak area between the 2009 and 2010 samples was not statistically significant ($p=0.26$), however, the difference between these years and samples from 2011 was statistically significant. The sulfur-related ion ($^{80}SO_3^-$) also trended with the percentage of dust, and was particularly high in the 2011 samples due to the presence of the calcium-rich dust. The phosphate ion ($^{79}PO_3^-$) generally trended with the percentage of biological residues. However, many dust residues also contained solely phosphate. For the OC residues, the mass spectral ion marker that represents oxidized OC ($^{43}C_2H_3O/CHNO^+$) (Qin et al., 2012) followed the percentage of OC residues. Amines are common OC particles that contain species such as $^{86}C_2H_2/(C_2H_5)_2NCH_2^+$ using ATOFMS, and are indicative of agricultural emissions from the California Central Valley (CV) (Creamean et al., 2011; Sorooshian et al., 2008). Amines were highest in the 2010 samples compared to 2009 and 2011, suggesting the 2010 residues were generally affected by local emissions from the CV. In order to investigate if SS was

potentially dissolving and mixing with particular residues, and as a follow up to the control experiments, one of the common ions used for SS ($^{93}NaCl_2^-$) was investigated (Gaston et al., 2011). The relative ion peak area of this ion is not shown in Fig. 6 due to lack of statistical significance, however, the percentage of residues containing this ion enables us to investigate the inter-annual trends. The chloride ion ($^{35,37}Cl^-$) was excluded from analysis because it can originate from mineral dust or biomass burning (Silva et al., 1999), or it can signify heterogeneous uptake of chloride by dust via reaction with $HCl_{(g)}$ (Sullivan et al., 2007b). Overall, 59 ± 1%, 38 ± 1% and 42 ± 1% of the total residues from 2009, 2010 and 2011, respectively, contained sodium chloride cluster ions. Of those, 75 ± 2%, 64 ± 3%, and 56 ± 3% were dust residues, as shown in Fig. 6i. One possible explanation is that the dust was processed in a marine environment during long-range transport from Asia (Suski, 2014; Zhang et al., 2003; Zhang & Iwasaka, 2004). However, it is more likely that raindrops or snowflakes containing the long-range transported dust residues were rimed with water droplets from a marine environment during descent, based on the findings of Creamean et al. (2013) from CalWater I.

Overall, the detailed results presented herein provide information regarding the striking interannual variability in the precipitation residue composition from each winter sampling season at SPD. The precipitation residues were predominantly a mix of dust and OC in 2009, as shown by higher percentages of OC and dust, and highest average relative ion peak area of oxidized OC. The samples from 2009 were also not highly influenced from biological sources, as shown by the lowest percentage of biological residues and lowest relative ion peak area of phosphate. Further, 2009 precipitation likely had more of a marine influence as shown by the highest percentage of residues mixed with $^{93}NaCl_2^-$ (59%), particularly with dust (75%). The 2010 samples were characterized by higher percentages of OC (50% on average), in particular amines (highest relative ion peak are of the amine ion), and had the lowest influence from dust as shown by the "%Dust" and the aluminosilicate ion marker. We detected the most dust, particularly the calcium-rich dust, in the 2011 precipitation samples, as shown by the percentage of these residues and the average relative ion peak areas of the aluminosilicate and sulfur-related ions. Residues other than the calcium-rich subtype in 2011 appeared to contain more biological material, i.e., were more "biological like," as shown by the phosphate ion. Overall, the samples from 2009 and 2011 were likely influenced by long-range transport, while the samples from 2010 were likely influenced by more local sources. Aircraft measurements of cloud residues support the vast difference in the aerosol composition from 2011; dust influenced clouds earlier in the study while biological material influenced clouds later in the study (Creamean et al., 2013). Further, these results support those of Suski (2014) and Suski et al. (2014), which demonstrate the omnipresence of mixed dust and biological particles in clouds during CalWater I and the importance of dust and particularly biological components in forming cloud ice.

3.4. Atmospheric implications: IN measurements of soil and precipitation residues

Determining the freezing temperatures of select control and precipitation samples provided insight into the ice nucleation properties of the residues. Based on our results, the residue chemistry and IN signatures lead us to believe the residues likely served as cloud nuclei as opposed to being scavenged by falling precipitation. Figure 7 shows results from the IN measurements of Asian 1 (Dunhuang), Asian 2 (YaDan), an almost pure kaolinite sample, and select precipitation samples. Samples containing predominantly dust and biological residues were the focus, as both aerosol types have been shown to provide contrasting sources of IN, one predominantly mineral and the other biological (Conen et al., 2011; Creamean et al., 2013; Field et al., 2006; Hoose & Mohler, 2012; Pratt et al., 2009). For the precipitation samples, the goal was to acquire IN measurements of samples that contained the highest ratios of dust to biological residues, as well as the highest ratios of each biological residue type to dust residues. Thus, Fig. 7 includes samples possessing the highest ratio of dust—particularly calcium-rich dust—to all biological residues (19:1, "Ca-dust:Bio"), the highest ratio of Bio 1 to all dust residues (6:1, "Bio 1:Dust"), and of Bio 2 to all dust residues (6:1, "Bio 2:Dust").

Some particle components within the Asian 1 sample activated ice formation as warm as −5.6 °C, and after heat treatment the IN concentrations decreased at temperatures warmer than −10 °C, suggesting the sample contained some amount of active biological IN of proteinaceous origin. This is consistent with the ATOFMS analysis (shown in the SM) which indicates the presence of biological material in the soil. These results suggest that some of the particles could have been active as IN under conditions relevant to the mixed-phase clouds during CalWater I. The Asian 2 sample contained ~10 times more IN overall compared to Asian 1, and contained more biological ice nucleating particles active above −15 °C as shown by the large difference between the natural and heated samples. Kaolin showed the least IN-active particles compared to the Asian soil samples, and was unaffected by heating. Interestingly, the Asian 2 sample also contained the highest relative abundance of the phosphate ion compared to the Asian 1, while kaolin had the lowest abundance (although values were within error, see SM). This trend suggests the presence of biological material within the dusts increased their ice nucleating abilities, supporting previous observations from Conen et al. (2011). Further, O'Sullivan et al. (2014) and Suski et al. (2014) demonstrated how biological components in mixed dust and biological particles dominate ice formation at warmer temperatures (> −15 °C).

The Bio 2:Dust sample had detectable numbers of IN at −5.6 °C; −4° to −6 °C in the typical upper temperature limit of IN activity in precipitation samples (Christner et al., 2008a; Vali, 1978). IN concentrations active at the warmest temperatures significantly decreased after heat treatment. In contrast, the Ca-dust:Bio sample did not show a large change after heat treatment. Accordingly, it contained minimal biological material, as confirmed by the ATOFMS data. The Bio 1: Dust sample had much lower IN concentrations in the precipitation water volume at temperatures warmer than −20 °C, and a lower onset temperature at which IN became detectable (i.e., only one well, out of 48 wells of 80 μL wells of a 20-fold

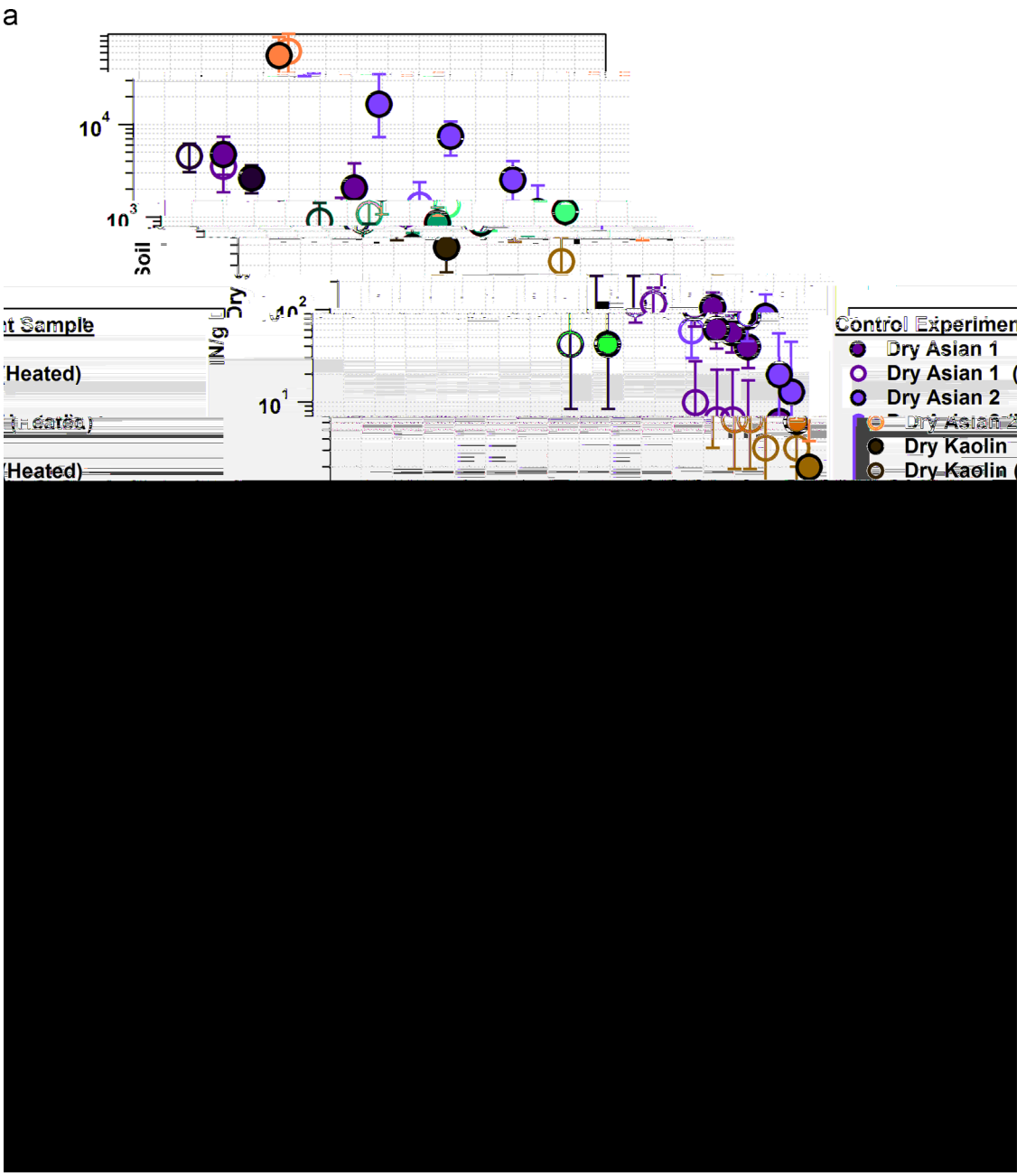

Fig. 7. IN immersion freezing analysis from dry soil and select precipitation samples: (a) IN measurements for the dry Asian 1, Asian 2, and kaolinite samples, and (b) Ca-dust:Bio (2011), Bio 1:Dust (2011), and Bio 2:Dust (2010). Some precipitation samples were filter concentrated to increase detection sensitivity at warmer temperatures, and these are shown as solid squares. Samples that were heat treated to denature biological IN are shown as open circles, and samples that were both filtered and heat treated are shown as open squares.

filter concentrate, froze at −8.7 °C and none froze at that temperature in the heat treated sample); these low levels prevented measurement of the biological contribution above −12 °C. O'Sullivan et al. (2014) and Tobo et al. (2014) found that soils with higher biological OC content were more IN active compared to the mineral components. Interestingly, the Bio 2 residues contained markers for OC as shown in Fig. 1e and were more IN active compared to the Bio 1 residues which contained little to no OC (Fig. 1d), thus supporting results from O'Sullivan et al. (2014) and Tobo et al. (2014). Overall, IN measurements of the dust and biological residues, and dry soil samples, corroborate that some proportion of the particles had the ability to serve as IN, supporting the original hypothesis that the precipitation residues served as IN. Purely biological residues contained a variety of high and low temperature IN. However, dust mixed with biological material tended to be more IN active as shown by the Asian soil IN measurements, emphasizing the importance of biological components in dust as sites of ice nucleation (Suski et al., 2014; Suski, 2014).

4. Conclusions

A combination of laboratory control experiments of known standards and observations of precipitation residue chemistry are presented herein. Based on the combination of the findings, this study provides detailed chemical information on the types of aerosols that are involved in cloud and precipitation processes. The control experiments serve as proxies for classifications of precipitation residues and support results from past studies of insoluble precipitation residues (Ault et al., 2011; Creamean et al., 2013). The sea salt solubility control experiment demonstrated that when sea salt is aerosolized from dilute solutions, residues are too small to be detected by the ATOFMS, therefore its presence in the precipitation samples collected during CalWater I cannot be ruled out on the basis of ATOFMS spectra. Dust was a major type of insoluble precipitation residue which was likely long-range transported from Asia, as demonstrated by the SPD soil control experiment and chemical similarity between the calcium-rich dust precipitation residue and the Asian soil samples. In addition, IN measurements of select precipitation and dry soil samples revealed that the ability to form cloud ice at temperatures above $-15\ ^{\circ}C$ was highly dependent on the presence of heat sensitive biological components in the dust residues.

The ability to confidently identify the chemical composition of particles in precipitation is important for understanding aerosol cloud droplet/crystal nucleation and wet removal mechanisms. IN measurements demonstrated that dust and biological residues likely served as ice nucleating cloud seeds as opposed to being scavenged by falling precipitation. The methods and techniques for precipitation residue classifications discussed herein can be applied to future studies. Further, when used in combination with meteorological and cloud microphysical property measurements, and ice nucleation measurements, precipitation residue chemistry can help determine the types of aerosols that are incorporated into clouds and which impact the formation of precipitation.

Acknowledgments

Funding for precipitation sample collection and chemical analysis was provided by the California Energy Commission, United States under contract UCOP/CIEE C-09-07 and CEC 500-09-043. J. Creamean was supported by the National Research Council Research Associateship Program (Contract number EA133F-10-CN-0187) for precipitation sample data interpretation, control experiment sample preparation, chemical analysis and interpretation, and for writing of the manuscript. T. Hill was supported by NSF, United States grant ATM-0841542 for ice nuclei measurements. The authors gratefully acknowledge J. Mayer, D. Collins, J. Cahill, M. Zauscher, E. Fitzgerald, and M. Moore from UCSD for assistance with equipment preparation and setup at SPD. We also thank M. Pickett from UCSD for assistance with running some of the control experiments, and C. Gaston and K. Suski for the IC measurements. The deployment of the NOAA and UCSD/SIO equipment at SPD involved many field staff, particularly C. King (NOAA/ESRL). The Forest Hill Power Utility District is acknowledged for hosting the sampling site at SPD. P. Neiman is acknowledged for their insightful discussions during preparation of this manuscript.

Appendix A. Supplementary material

Supplementary data associated with this article can be found in the online version at: http://dx.doi.org/10.1016/j.jaerosci.2014.05.005.

References

Allen, J.O. (2004). *Quantitative analysis of aerosol time-of-flight mass spectrometry data using YAADA. In Book Quantitative Analysis of Aerosol Time-of-Flight Mass Spectrometry Data using YAADA*. Arizona State University: Phoenix, AZ, USA.

Andreae, M.O., Charlson, R.J., Bruynseels, F., Storms, H., Vangrieken, R., & Maenhaut, W. (1986). Internal mixture of sea salt, silicates, and excess sulfate in marine aerosols. *Science*, *232*, 1620–1623.

Andreae, M.O., Talbot, R.W., Berresheim, H., & Beecher, K.M. (1990). Precipitation chemistry in central Amazonia. *Journal of Geophysical Research—Atmospheres*, *95*, 16987–16999.

Ault, A.P., Williams, C.R., White, A.B., Neiman, P.J., Creamean, J.M., Gaston, C.J., Ralph, F.M., & Prather, K.A. (2011). Detection of Asian dust in California orographic precipitation. *Journal of Geophysical Research—Atmospheres*, *116*, 16205–16220, http://dx.doi.org/10.1029/2010JD015351.

Brahney, J., Ballantyne, A.P., Sievers, C., & Neff, J.C. (2013). Increasing Ca^{2+} deposition in the western US: the role of mineral aerosols. *Aeolian Research*, *10*, 77–87.

Bruintjes, R.T. (1999). A review of cloud seeding experiments to enhance precipitation and some new prospects. *Bulletin of the American Meteorological Society*, *80*, 805–820.

Burge, H.A., & Solomon, W.R. (1987). Sampling and analysis of biological aerosols. *Atmospheric Environment*, *21*, 451–456.

Christner, B.C., Cai, R., Morris, C.E., McCarter, K.S., Foreman, C.M., Skidmore, M.L., Montross, S.N., & Sands, D.C. (2008a). Geographic, seasonal, and precipitation chemistry influence on the abundance and activity of biological ice nucleators in rain and snow. *Proceedings of the National Academy of Sciences of the United States of America*, *105*, 18854–18859.

Christner, B.C., Morris, C.E., Foreman, C.M., Cai, R.M., & Sands, D.C. (2008b). Ubiquity of biological ice nucleators in snowfall. *Science*, *319*, 1214.

Conen, F., Morris, C.E., Leifeld, J., Yakutin, M.V., & Alewell, C. (2011). Biological residues define the ice nucleation properties of soil dust. *Atmospheric Chemistry and Physics*, *11*, 9643–9648.

Creamean, J.M., Ault, A.P., Ten Hoeve, J.E., Jacobson, M.Z., Roberts, G.C., & Prather, K.A. (2011). Measurements of aerosol chemistry during new particle formation events at a remote rural mountain site. *Environmental Science and Technology*, *45*, 8208–8216.

Creamean, J.M., Suski, K.J., Rosenfeld, D., Carzola, A., DeMott, P.J., Sullivan, R.C., White, A.B., Ralph, F.M., Minnis, P., Comstock, J.M., Tomlinson, J.M., & Prather, K.A. (2013). Dust and biological aerosols from the Sahara and Asia influence precipitation in the Western US. *Science*, *339*, 1572–1578.

DeMott, P.J., Sullivan, R.C., Ruppel, M.J., Hill, T.C., Mason, R., Ault, A.P., Prather, K.A., Collins, D.B., Kim, M.J., Bertram, A.K., Bertram, T.H., Grassian, V.H., & Franc, G.D. (2013). Laboratory measurements of ice nuclei concentrations from ocean water spray. In: *Nucleation and atmospheric aerosols, 19th International Conference, AIP Conference Proceedings, Book Laboratory Measurements of Ice Nuclei Concentrations from Ocean Water Spray*, City, American Institute of Physics, Fort Collins, CO, USA, vol. 1527, pp. 941–944.

Dentener, F.J., Carmichael, G.R., Zhang, Y., Lelieveld, J., & Crutzen, P.J. (1996). Role of mineral aerosol as a reactive surface in the global troposphere. *Journal of Geophysical Research—Atmospheres*, *101*, 22869–22889.

Dunlea, E.J., DeCarlo, P.F., Aiken, A.C., Kimmel, J.R., Peltier, R.E., Weber, R.J., Tomlinson, J., Collins, D.R., Shinozuka, Y., McNaughton, C.S., Howell, S.G., Clarke, A.D., Emmons, L.K., Apel, E.C., Pfister, G.G., van Donkelaar, A., Martin, R.V., Millet, D.B., Heald, C.L., & Jimenez, J.L. (2009). Evolution of Asian aerosols during transpacific transport in INTEX-B. *Atmospheric Chemistry and Physics*, *9*, 7257–7287.

Facchini, M.C., Rinaldi, M., Decesari, S., Carbone, C., Finessi, E., Mircea, M., Fuzzi, S., Ceburnis, D., Flanagan, R., Nilsson, E.D., de Leeuw, G., Martino, M., Woeltjen, C.D., & O'Dowd, C.D. (2008). Primary submicron marine aerosol dominated by insoluble organic colloids and aggregates. *Geophysical Research Letters*, 35.

Fergenson, D.P., Pitesky, M.E., Tobias, H.J., Steele, P.T., Czerwieniec, G.A., Russell, S.C., Lebrilla, C.B., Horn, J.M., Coffee, K.R., Srivastava, A., Pillai, S.P., Shih, M.T.P., Hall, H.L., Ramponi, A.J., Chang, J.T., Langlois, R.G., Estacio, P.L., Hadley, R.T., Frank, M., & Gard, E.E. (2004). Reagentless detection and classification of individual bioaerosol particles in seconds. *Analytical Chemistry*, *76*, 373–378.

Fernandez, I., Cabaneiro, A., & Carballas, T. (1997). Organic matter changes immediately after a wildfire in an Atlantic forest soil and comparison with laboratory soil heating. *Soil Biology & Biochemistry*, *29*, 1–11.

Field, P.R., Mohler, O., Connolly, P., Kramer, M., Cotton, R., Heymsfield, A.J., Saathoff, H., & Schnaiter, M. (2006). Some ice nucleation characteristics of Asian and Saharan desert dust. *Atmospheric Chemistry and Physics*, *6*, 2991–3006.

Garcia, E., Hill, T.C.J., Prenni, A.J., DeMott, P.J., Franc, G.D., & Kreidenweis, S.M. (2012). Biogenic ice nuclei in boundary layer air over two U.S. High Plains agricultural regions. *Journal of Geophysical Research-Atmospheres*, *117*, 18209–18221.

Gard, E., Mayer, J.E., Morrical, B.D., Dienes, T., Fergenson, D.P., & Prather, K.A. (1997). Real-time analysis of individual atmospheric aerosol particles: design and performance of a portable ATOFMS. *Analytical Chemistry*, *69*, 4083–4091.

Gaston, C.J., Furutani, H., Guazzotti, S.A., Coffee, K.R., Bates, T.S., Quinn, P.K., Aluwihare, L.I., Mitchell, B.G., & Prather, K.A. (2011). Unique ocean-derived particles serve as a proxy for changes in ocean chemistry. *Journal of Geophysical Research—Atmospheres*, *116* 18310–13323.

Hao, L., Romakkaniemi, S., Kortelainen, A., Jaatinen, A., Portin, H., Miettinen, P., Komppula, M., Leskinen, A., Virtanen, A., Smith, J.N., Sueper, D., Worsnop, D.R., Lehtinen, K.E.J., & Laaksonen, A. (2013). Aerosol chemical composition in cloud events by high resolution time-of-flight aerosol mass spectrometry. *Environmental Science and Technology*, *47*, 2645–2653.

Hegg, D.A., Gao, S., Hoppel, W., Frick, G., Caffrey, P., Leaitch, W.R., Shantz, N., Ambrusko, J., & Albrechcinski, T. (2001). Laboratory studies of the efficiency of selected organic aerosols as CCN. *Atmospheric Research*, *58*, 155–166.

Holecek, J.C., Spencer, M.T., & Prather, K.A. (2007). Analysis of rainwater samples: comparison of single particle residues with ambient particle chemistry from the northeast Pacific and Indian oceans. *Journal of Geophysical Research-Atmospheres*, *112* 22S24–22S34.

Hongve, D., van Hees, P.A.W., & Lundstrom, U.S. (2000). Dissolved components in precipitation water percolated through forest litter. *European Journal of Soil Science*, *51*, 667–677.

Hoose, C., & Mohler, O. (2012). Heterogeneous ice nucleation on atmospheric aerosols: a review of results from laboratory experiments. *Atmospheric Chemistry and Physics*, *12*, 9817–9854.

Huntington, T.G. (2006). Evidence for intensification of the global water cycle: review and synthesis. *Journal of Hydrology*, *319*, 83–95.

Jaenicke, R. (2005). Abundance of cellular material and proteins in the atmosphere. *Science*, *308*, 73.

Krueger, B.J., Grassian, V.H., Cowin, J.P., & Laskin, A. (2004). Heterogeneous chemistry of individual mineral dust particles from different dust source regions: the importance of particle mineralogy. *Atmospheric Environment*, *38*, 6253–6261.

Kumar, P., Nenes, A., & Sokolik, I.N. (2009). Importance of adsorption for CCN activity and hygroscopic properties of mineral dust aerosol. *Geophysical Research Letters*, *36*, 24804–24810.

Kumar, P.P., Broekhuizen, K., & Abbatt, J.P.D. (2003). Organic acids as cloud condensation nuclei: laboratory studies of highly soluble and insoluble species. *Atmospheric Chemistry and Physics*, *3*, 509–520.

Levi, Y., & Rosenfeld, D. (1996). Ice nuclei, rainwater chemical composition, and static cloud seeding effects in Israel. *Journal of Applied Meteorology*, *35*, 1494–1501.

Li, Y.H., Wang, Y., Ding, A.J., Liu, X.H., Guo, J., Li, P.H., Sun, M.H., Ge, F.L., & Wang, W.X. (2011). Impact of long-range transport and under-cloud scavenging on precipitation chemistry in East China. *Environmental Science and Pollution Research*, *18*, 1544–1554.

Ma, C.J., Tohno, S., Kasahara, M., & Hayakawa, S. (2004). Properties of the size-resolved and individual cloud droplets collected in western Japan during the Asian dust storm event. *Atmospheric Environment*, *38*, 4519–4529.

Matthias-Maser, S., Bogs, B., & Jaenicke, R. (2000). The size distribution of primary biological aerosol particles in cloud water on the mountain Kleiner Feldberg/Taunus(FRG). *Atmospheric Research*, *54*, 1–13.

Moffet, R.C., Henn, T.R., Tivanski, A.V., Hopkins, R.J., Desyaterik, Y., Kilcoyne, A.L.D., Tyliszczak, T., Fast, J., Barnard, J., Shutthanandan, V., Cliff, S.S., Perry, K.D., Laskin, A., & Gilles, M.K. (2010). Microscopic characterization of carbonaceous aerosol particle aging in the outflow from Mexico City. *Atmospheric Chemistry and Physics*, *10*, 961–976.

Muhlbauer, A., & Lohmann, U. (2009). Sensitivity studies of aerosol–cloud interactions in mixed-phase orographic precipitation. *Journal of the Atmospheric Sciences*, *66*, 2517–2538.

Murray, B.J., O'Sullivan, D., Atkinson, J.D., & Webb, M.E. (2012). Ice nucleation by particles immersed in supercooled cloud droplets. *Chemical Society Reviews*, *41*, 6519–6554.

Noguchi, I., & Hara, H. (2004). Ionic imbalance due to hydrogen carbonate from Asian dust. *Atmospheric Environment*, *38*, 6969–6976.

O'Dowd, C.D., Smith, M.H., Consterdine, I.E., & Lowe, J.A. (1997). Marine aerosol, sea-salt, and the marine sulphur cycle: a short review. *Atmospheric Environment*, *31*, 73–80.

O'Sullivan, D., Murray, B.J., Malkin, T.L., Whale, T., Umo, N.S., Atkinson, J.D., Price, H.C., Baustian, K.J., Browse, J., & Webb, M.E. (2014). Ice nucleation by fertile soil dusts: relative importance of mineral and biogenic components. *Atmospheric Chemistry and Physics*, *14*, 1853–1867.

Okada, K., Naruse, H., Tanaka, T., Nemoto, O., Iwasaka, Y., Wu, P.M., Ono, A., Duce, R.A., Uematsu, M., Merrill, J.T., & Arao, K. (1990). X-ray spectrometry of individual Asian dust-storm particles over the Japanese Islands and the North Pacific-Ocean. *Atmospheric Environment a-General*, *24*, 1369–1378.

Petters, M.D., Carrico, C.M., Kreidenweis, S.M., Prenni, A.J., DeMott, P.J., Collett, J.L., & Moosmuller, H. (2009). Cloud condensation nucleation activity of biomass burning aerosol. *Journal of Geophysical Research—Atmospheres*, *114*, 22205–22221.

Pósfai, M., Gelencsér, A., Simonics, R., Arató, K., Li, J., Hobbs, P.V., & Buseck, P.R. (2004). Atmospheric tar balls: particles from biomass and biofuel burning. *Journal of Geophysical Research—Atmospheres*, *109*, 6213–6222.

Prather, K.A., Bertram, T.H., Grassian, V.H., Deane, G.B., Stokes, M.D., DeMott, P.J., Aluwihare, L.I., Palenik, B.P., Azam, F., Seinfeld, J.H., Moffet, R.C., Molina, M.J., Cappa, C.D., Geiger, F.M., Roberts, G.C., Russell, L.M., Ault, A.P., Baltrusaitis, J., Collins, D.B., Corrigan, C.E., Caudra-Rodriguez, L.A., Ebben, C.J., Forestieri, S.D., Guasco, T.L., Hersey, S.P., Kim, M.J., Lambert, W.F., Modini, R.L., Mui, W., Pedler, B.E., Ruppel, M.J., Ryder, O.S., Schoepp, N.G., Sullivan, R.C., & Zhao, D. (2013). Bringing the ocean into the laboratory to probe the chemical complexity of sea spray aerosol. *Proceedings of the National Academy of Sciences of the Unites States of America*, *110*, 7550–7555.

Pratt, K.A., DeMott, P.J., French, J.R., Wang, Z., Westphal, D.L., Heymsfield, A.J., Twohy, C.H., Prenni, A.J., & Prather, K.A. (2009). in situ detection of biological particles in cloud ice-crystals. *Nature Geoscience*, *2*, 397–400.

Pruppacher, H.R., & Klett, J.D. (1978). *Microphysics of Clouds and Precipitation*. Taylor & Francis: Dordecht, The Netherlands.
Qin, X.Y., & Prather, K.A. (2006). Impact of biomass emissions on particle chemistry during the California Regional Particulate Air Quality Study. *International Journal of Mass Spectrometry*, *258*, 142–150.
Qin, X.Y., Pratt, K.A., Shields, L.G., Toner, S.M., & Prather, K.A. (2012). Seasonal comparisons of single-particle chemical mixing state in Riverside, CA. *Atmospheric Environment*, *59*, 587–596.
Rosenfeld, D. (2000). Suppression of rain and snow by urban and industrial air pollution. *Science*, *287*, 1793–1796.
Rosenfeld, D., Lohmann, U., Raga, G.B., O'Dowd, C.D., Kulmala, M., Fuzzi, S., Reissell, A., & Andreae, M.O. (2008). Flood or drought: how do aerosols affect precipitation?. *Science*, *321*, 1309–1313.
Rosenfeld, D., Rudich, Y., & Lahav, R. (2001). Desert dust suppressing precipitation: a possible desertification feedback loop. *Proceedings of the National Academy of Sciences of the United States of America*, *98*, 5975–5980.
Schnitzer, M., & Khan, S.U. (1978). Soil organic matter. Developments in Soil Science. In A.B. McBratney, & A.E. Hartemink (Eds.), *Book Soil Organic Matter (8th ed.)*. Elsevier Science Publishers B.V.: Wageningen, The Netherlands.
Schutz, L., & Kramer, M. (1987). Rainwater composition over a rural area with special emphasis on the size distribution of insoluble particulate matter. *Journal of Atmospheric Chemistry*, *5*, 173–184.
Silva, P.J. (2000). *Source Profiling and Apportionment of Airborne Particles: A New Approach Using Aerosol Time-of-Flight Mass Spectrometry*. University of California, Riverside: Riverside.
Silva, P.J., Liu, D.Y., Noble, C.A., & Prather, K.A. (1999). Size and chemical characterization of individual particles resulting from biomass burning of local Southern California species. *Environmental Science & Technology*, *33*, 3068–3076.
Song, X.H., Hopke, P.K., Fergenson, D.P., & Prather, K.A. (1999). Classification of single particles analyzed by ATOFMS using an artificial neural network, ART-2A. *Analytical Chemistry*, *71*, 860–865.
Sorooshian, A., Murphy, S.N., Hersey, S., Gates, H., Padro, L.T., Nenes, A., Brechtel, F.J., Jonsson, H., Flagan, R.C., & Seinfeld, J.H. (2008). Comprehensive airborne characterization of aerosol from a major bovine source. *Atmospheric Chemistry and Physics*, *8*, 5489–5520.
Spracklen, D.V., Arnold, S.R., Sciare, J., Carslaw, K.S., & Pio, C. (2008). Globally significant oceanic source of organic carbon aerosol. *Geophysical Research Letters*, *35*, 12811–12816.
Sullivan, R.C., Guazzotti, S.A., Sodeman, D.A., & Prather, K.A. (2007a). Direct observations of the atmospheric processing of Asian mineral dust. *Atmospheric Chemistry and Physics*, *7*, 1213–1236.
Sullivan, R.C., Guazzotti, S.A., Sodeman, D.A., Tang, Y.H., Carmichael, G.R., & Prather, K.A. (2007b). Mineral dust is a sink for chlorine in the marine boundary layer. *Atmospheric Environment*, *41*, 7166–7179.
Sullivan, R.C., Moore, M.J.K., Petters, M.D., Kreidenweis, S.M., Qafoku, O., Laskin, A., Roberts, G.C., & Prather, K.A. (2010). Impact of particle generation method on the apparent hygroscopicity of insoluble mineral particles. *Aerosol Science and Technology*, *44*, 830–846.
Sullivan, R.C., Moore, M.J.K., Petters, M.D., Kreidenweis, S.M., Roberts, G.C., & Prather, K.A. (2009a). Effect of chemical mixing state on the hygroscopicity and cloud nucleation properties of calcium mineral dust particles. *Atmospheric Chemistry and Physics*, *9*, 3303–3316.
Sullivan, R.C., Moore, M.J.K., Petters, M.D., Kreidenweis, S.M., Roberts, G.C., & Prather, K.A. (2009b). Timescale for hygroscopic conversion of calcite mineral particles through heterogeneous reaction with nitric acid. *Physical Chemistry Chemical Physics*, *11*, 7826–7837.
Sullivan, R.C., & Prather, K.A. (2007). Investigations of the diurnal cycle and mixing state of oxalic acid in individual particles in Asian aerosol outflow. *Environmental Science & Technology*, *41*, 8062–8069.
Sun, J.M., & Ariya, P.A. (2006). Atmospheric organic and bio-aerosols as cloud condensation nuclei (CCN): a review. *Atmospheric Environment*, *40*, 795–820.
Sun, M.H., Wang, Y., Wang, T., Fan, S.J., Wang, W.X., Li, P.H., Guo, J., & Li, Y.H. (2010). Cloud and the corresponding precipitation chemistry in south China: water-soluble components and pollution transport. *Journal of Geophysical Research—Atmospheres*, *115*, 22303–22313.
Suski, K.J. (2014). *In-Situ Measurements of Dust, Soot, and Biological Species and their Effects on Mixed Phase Clouds*. University of California-San Diego: La Jolla.
Suski, K.J., Rosenfeld, D., Anderson, J.R., Twohy, C.H., Heymsfield, A.J., & Prather, K.A. (2014). Biological species dominate ice nucleation in marine clouds warmer than $-15\ ^{\circ}C$. *Nature Geoscience* (in preparation).
Tobo, Y., DeMott, P.J., Hill, T.C.J., Prenni, A.J., Swoboda-Colberg, N.G., Franc, G.D., & Kreidenweis, S.M. (2014). Organic matter matters for ice nuclei of agricultural soil origin. *Atmospheric Chemistry and Physics Discussion*, *14*, 9705–9728, http://dx.doi.org/10.5194/acpd-14-9705-2014.
Vaïtilingom, M., Amato, P., Sancelme, M., Laj, P., Leriche, M., & Delort, A.M. (2010). Contribution of microbial activity to carbon chemistry in clouds. *Applied and Environmental Microbiology*, *76*, 23–29.
Vali, Gabor (1971). Quantitative Evaluation of Experimental Results an the Heterogeneous Freezing Nucleation of Supercooled Liquids. *Journal of Atmospheric Science*, *28*, 402–409.
Vali, G. (1978). Freezing nucleus content of hail and rain in NE Colorado. *American Meterological Society Monograph*, *38*, 93–105.
Vlasenko, A., Sjogren, S., Weingartner, E., Gaggeler, H.W., & Ammann, M. (2005). Generation of submicron Arizona test dust aerosol: chemical and hygroscopic properties. *Aerosol Science and Technology*, *39*, 452–460.
Yang, F., Tan, J., Shi, Z.B., Cai, Y., He, K., Ma, Y., Duan, F., Okuda, T., Tanaka, S., & Chen, G. (2012). Five-year record of atmospheric precipitation chemistry in urban Beijing, China. *Atmospheric Chemistry and Physics*, *12*, 2025–2035.
Zhang, C., Wu, G., Gao, S., Zhao, Z., Zhang, X., Tian, L., Mu, Y., & Joswiak, D. (2013). Distribution of major elements between the dissolved and insoluble fractions in surface snow at Urumqi Glacier No. 1, Eastern Tien Shan. *Atmospheric Research*, *132–133*, 299–308.
Zhang, D.Z., & Iwasaka, Y. (2004). Size change of Asian dust particles caused by sea salt interaction: measurements in southwestern Japan. *Geophysical Research Letters*, *31*, 15102–15106.
Zhang, D.Z., Iwasaka, Y., Shi, G.Y., Zang, J.Y., Matsuki, A., & Trochkine, D. (2003). Mixture state and size of Asian dust particles collected at southwestern Japan in spring 2000. *Journal of Geophysical Research-Atmospheres*, *108*, 4670–4682.